Published in final edited form as:
J Comp Neurol. 2011 January 1; 519(1): 148–161. doi:10.1002/cne.22510.

Organization and development of zebra finch HVC and paraHVC based on expression of *zRalDH*, an enzyme associated with retinoic acid production

Christopher R. Olson, **Paulo Vianney Rodrigues**[1], **Jin Kwon Jeong**[2], **Daniel J. Prahl**[3], and **Claudio V. Mello**
Department of Behavioral Neuroscience, Oregon Health and Science University, 3181 SW Sam Jackson Park Road, Portland, OR 97239

Abstract

The *zRalDH* gene encodes an aldehyde dehydrogenase associated with the conversion of retinaldehyde (the main vitamin A metabolite) into retinoic acid and its expression is highly enriched in the song control system of adult zebra finches (*T. gutatta*). Within song control nucleus HVC, *zRalDH* is specifically expressed in the neurons that project to area X of the striatum. It is also expressed in paraHVC, commonly considered a medial extension of HVC that is closely associated with auditory areas in the caudomedial telencephalon. Here we used *in situ* hybridization to generate a detailed analysis of HVC and paraHVC based on expression of *zRalDH* for adult zebra finches of both sexes and for males during the song learning period. We demonstrate that the distribution of *zRalDH*-positive cells can be used for accurate assessments of HVC and paraHVC in adult and juvenile males. We describe marked developmental changes in the numbers of *zRalDH*-expressing cells in HVC and paraHVC, reaching a peak at day 50 post-hatch, an effect potentially due to dynamic changes in the population of X-projecting cells in HVC. We also show that *zRalDH*-expressing cells in adult females, although much less numerous than in males, have a surprisingly broad distribution along the medial-to-lateral extent of HVC but are lacking where paraHVC is found in adult males. Our study thus contributes to our understanding of the nuclear organization of the song system and the dynamics of its developmental changes during the song learning period.

Keywords

retinaldehyde dehydrogenase; songbird; vocal learning; song maturation; sex differences; *in situ* hybridization

Introduction

The song of the zebra finch (*Taeniopygia guttata*) is a complex, learned behavior that is acquired at an early age from an adult tutor, practiced during a period when auditory feedback has a modulatory effect on vocal-motor programs, and refined to a stereotyped

Corresponding author: Claudio V. Mello, Department of Behavioral Neuroscience, Oregon Health and Science University, 3181 SW Sam Jackson Park Road, Portland, OR 97239 (phone) 503-418-2650, (fax) 503-494-6877, melloc@ohsu.edu.
[1]Current address: Department of Otorhinolaryngology: Head and Neck Surgery, University of Pennsylvania School of Medicine, 3400 Spruce - 5 Ravdin, Philadelphia, PA 19104
[2]Current address: Meliora 117, Brain & Cognitive Sciences, University of Rochester, Rochester, NY 14627-0268
[3]Current address: Department of Biology, University of Portland, 5000 N. Willamette Blvd., Portland, OR 97203

Suggested Associate Editor: Dr. John L. R. Rubenstein, University of California–San Francisco: Developmental Neurobiology

stage that is maintained in adulthood (Zeigler and Marler, 2004; Zeigler and Marler, 2008). Song is controlled by a series of discrete brain nuclei that occur in two interconnected pathways originating in nucleus HVC (a proper name; see Reiner et al. (2004) for nomenclature and Wild (1997) and Zeigler and Marler (2004) for connections). In the direct vocal-motor pathway, which is required for song production (Nottebohm et al., 1976), neurons from HVC project to the robust nucleus of the arcopallium (RA) and this circuit ultimately controls motor neurons that innervate respiratory muscles and the syrinx. In the anterior pathway projections from HVC innervate a loop consisting of the sequential projections from striatal area X to the dorsal lateral nucleus of the medial thalamus (DLM) from DLM to the lateral magnocellular nucleus of the anterior nidopallium (LMAN), and from LMAN to area X, thus closing the loop, or from LMAN to the direct pathway via RA. This anterior pathway is involved in song learning during the sensory-motor modulation phase, and lesions or pharmaceutical blocking of its nuclei reduces variability in juvenile song prematurely and inhibits learning ability (Bottjer et al., 1984; Kao and Brainard, 2006; Ölveczky et al., 2005; Scharff and Nottebohm, 1991; Sohrabji et al., 1990). The song control system provides a strong model for the experimental study of human vocal learning (Doupe and Kuhl, 1999), yet the molecular and cellular changes that occur during song learning remain to be fully described.

Throughout the song learning period the song control pathways are characterized by a high degree of neuronal plasticity that corresponds to changing patterns of gene expression (Clayton, 1997; Velho et al., 2007; Wada et al., 2006; Wissman and Brenowitz, 2009). Most notably, HVC volume and cell number increase dramatically during the song learning period (Bottjer et al., 1986). These developmental changes in HVC occur largely through a burst of post-natal neurogenesis of the RA-projecting cells (Alvarez-Buylla et al., 1988; Kirn and DeVoogd, 1989), but turnover of these cells continues through adulthood (Kirn et al., 1991). RA-projecting cells originate from a proliferative layer in the wall of the lateral ventricle dorsal to HVC (Alvarez-Buylla et al., 1998; Scott and Lois, 2007) and migrate into HVC where they are incorporated into the existing architecture (Alvarez-Buylla et al., 1988; Kirn et al., 1999; Scott and Lois, 2007). This incorporation of new neurons and a high turnover of cells in juveniles correlate with an increase in song syllable variability during the song learning period (Wilbrecht et al., 2006). In contrast, neurons that project to area X are born during the embryonic stage, but not during juvenile development or adulthood (Alvarez-Buylla et al., 1988; Kirn et al., 1999), and are thought to represent a stable population throughout life. These cells also occur in a structure that extends from HVC towards the midline and contains X-projecting neurons but not RA-projecting neurons (Bottjer et al., 1989; Denisenko-Nehrbass et al., 2000; Foster and Bottjer, 1998; Johnson and Bottjer, 1995). This medial extension to HVC (as originally described in Bottjer et al., 1989) or the paraHVC (as referred to since Johnson and Bottjer, 1995) has been suggested to undergo developmental changes during the song learning period, an intriguing possibility given its close proximity to the caudomedial nidopallium (NCM), an auditory area thought to be involved in aspects of song model acquisition in juveniles (Bolhuis et al., 2001; Bolhuis et al., 2000; London and Clayton, 2008; Phan et al., 2006). However, paraHVC remains a somewhat ill-defined region in terms of its full extent, cell composition and presence in juveniles and females. Furthermore, the extent to which paraHVC undergoes developmental changes has not yet been determined. This is a challenging question given the difficulty in clearly distinguishing between HVC and paraHVC, particularly in juveniles.

Retinoid signaling is important for the maintenance and differentiation of neuronal phenotypes (McCaffery and Drager, 2000; McCaffery et al., 2006) and changes that occur in its expression are likely to reflect key developmental processes in the brain. In the zebra finch, retinaldehyde-specific aldehyde dehydrogenase (*zRalDH*), the terminal enzyme in the metabolic pathway from Vitamin A to retinoic acid (Napoli, 1999), is highly enriched in

specific parts of the song system (Denisenko-Nehrbass et al., 2000). We use here "*zRalDH*" to be consistent with the previous songbird literature; however, this gene is also known as *ALDH1A2* based on the HUGO Gene Nomenclature Committee, or *RALDH2*. Within HVC, *zRalDH* is a reliable molecular marker for the large neurons that project to striatal area X, as it is selectively expressed in cells that can be labeled by retrograde tracer injections into area X (Denisenko-Nehrbass et al., 2000). In adults, *zRalDH* is also expressed in song nucleus LMAN, in the rostral nidopallium adjacent to LMAN, and in the hyperpallium. In juveniles, *zRalDH* is expressed in RA up to ~35 days post hatch (dph), but its expression in this song nucleus becomes undetectable by 50 dph (Denisenko-Nehrbass et al, 2000). In contrast to *zRalDH*, retinoic acid receptors (RARs) have a broad distribution that includes both *zRalDH*-positive and -negative cells, suggesting broad effects of retinoic acid in the songbird brain. Yet expression of RARs is highest in area X, the main target of the *zRalDH*-positive cells in HVC, and considerably high in NCM, located ventrally to paraHVC, and in HVC (Jeong et al., 2005).

Here we used *in situ* hybridization to describe in detail the organization and development of HVC and paraHVC in the zebra finch brain based on *zRalDH* expression. We examined adult males (>120 dph) with crystallized song, adult females, and juvenile males at 3 different ages (20, 35 and 50 dph), corresponding to different stages in the song learning period. Our results provide a clear and detailed definition of paraHVC, allowing us to clearly distinguish it from HVC in males and to demonstrate its absence in females. Most importantly, our data provide evidence for marked developmental changes in the population of *zRalDH*-expressing cells in HVC and paraHVC during the course of the song learning period. These findings are indicative of dynamic developmental changes in X-projecting neurons in HVC/paraHVC in concert with song learning, although further studies are required to differentiate between changes in the molecular phenotype versus the numbers of X-projecting cells in this part of the song system.

Methods

Animals

Pairs of zebra finches from our colony were established in individual cages and their nests were checked daily for hatching. Soon after hatching juveniles were marked with uniquely colored leg bands and were placed together in a common cage at ~25 dph for the older age groups. All birds were housed in a common room with visual and auditory access to other birds, including adult singing males. For this study we used males at 20, 35, 50 or >120 dph and females >120 dph of age; n = 4 per group. We chose three different juvenile ages that correspond, respectively, to an age that slightly precedes the critical period for the sensory acquisition of the song template (20 dph), the middle of the period of sensory acquisition and the beginning of the sensorimotor learning period (35 dph), and the middle of the sensorimotor period (50 dph). Birds were killed by decapitation, their brains quickly dissected and fresh frozen in Tissue-Tek with a dry ice/isopropanol slurry. For birds 35 days and older sex was identified by plumage characteristics, while for the 20 day-old birds sex was determined through PCR amplification of sex-specific bands from DNA extracted from blood or brain tissue samples using a previously established protocol for zebra finches (Griffiths et al., 1998). Parasagittal brain sections (10 μm intervals) were cut on a cryostat (up to ~4 mm lat, a range that adequately encompasses paraHVC and HVC. Sections were melted to microscope slides and stored at −80°C until ready for *in situ* hybridization. This work was approved by OHSU's IACUC committee in accordance with institutional and national guidelines.

In situ hybridization

Digoxigenin-labeled riboprobes were generated from *zRalDH* as described in (Wood et al., 2008). Briefly, using PCR amplification and sequence-specific primers with added overhangs containing T3 and T7 promoters, we generated a 538-bp fragment consisting of coding sequence extending from base pair 478 to 1016 of the cloned zebra finch *zRalDH* transcript (GenBank accession number AF162770). The primer sequences were 5′-TAATACGACTCACTATAGGGACAGCGTAGTC-3′ for T7, and 5′-ATTAACCCTCACTAAAGGGAGAATCACTGAACAGCG-3′, where the underlined text indicates the *zRalDH* coding sequences. The template was then generated through further PCR amplification of the initial fragment with generic T7 and T3 primers in 25 cycles of melting for 30 sec at 94°C, annealing for 45 sec at 67°, and elongation for 2 min at 72°, followed by a final elongation for 5 min at 72°. Following cleaning with a PCR purification kit, antisense riboprobes were generated from the PCR amplified DNA template with T7 RNA polymerase using a digoxigenin-UTP RNA labeling kit (Roche) at 37°C for 2 hrs. Riboprobes were then hybridized to brain sections following Mello et al. (1997) using an optimized non-radioactive detection protocol for DIG-labeled riboprobes, as detailed further in Lovell et al. (submitted). In short, sections were fixed in 3% phosphate-buffered paraformaldehyde for 5 min., followed by a brief rinse in 0.1 M PBS (pH = 7.4) and dehydration in an alcohol-series (70%, 95%, 100% for 2 min each). Sections were then acetylated for 10 min. (0.25% acetic anhydride in 1.4% triethanolamine and dH_2O), rinsed 3 times in 2x SSPE, and alcohol-series dehydrated. Hybridization solution (50% formamide, 2x SSPE, 2 μg/μl tRNA, 1 μg/μl BSA, 1 μg/μl Poly A, and the *zRalDH* riboprobe) was prepared and slides were coverslipped with 32 μl of solution per slide (~25 nl/μl of probe per slide) and immersed overnight in mineral oil at 65°C. The next day slides were rinsed in chloroform and coverslips were removed in 2x SSPE. Post-hybridization washes included 1 hr in 2x SSPE at RT, 1 hr in 2x SSPE plus 50% formamide at 65°C, and twice for 30 min in 0.1x SSPE at 65°C. Sections on slides were framed with a Dako Pen and endogenous peroxidase was quenched with 0.3% H_2O_2 in a 0.1 M Tris-0.15 M NaCl-0.3% Triton X-100 (TNT) buffer for 10 minutes, followed by 3 washes in TNT for 5 minutes each with agitation. Sections were then blocked with 8.3 ng/μl BSA in TNT (TNB, pH = 7.4) for 30 min, followed by incubation with a peroxidase-conjugated anti-digoxigenin antibody (1:100 dilution; Roche) in TNB for 2 hr. The digoxigenin-labeled *zRalDH* riboprobes were visualized by incubation with tyramide coupled to Alexa 488 (Molecular Probes). The method above was primarily used for the mapping and quantitative analysis shown on Figs. 3-7. Alternatively, we used a chromagen precipitation method to obtain a more permanent histological record of our preparations, as shown on Figs. 1 and 2. Briefly, after post-hybridization washes, the slides were briefly rinsed in TNT and tissue sections were framed with a Dako pen. Sections were blocked with TNB (200 μl per slide) for 2 hrs, and then incubated with anti-DIG alkaline phosphatase conjugated antibodies (1:300 dilution, Roche) in TNB for 2 hrs. The slides were then rinsed in TNT, and incubated with ~200 μl per slide of a solution containing 0.21 g/L 5-bromo-4-chloro-3indolyl-phosphate with 0.42 g/L nitroblue tetrazolium in tris buffer (BCIP/TNB; Perkin-Elmer) overnight at room temperature. Once *zRalDH*-positive cells were visible, slides were again rinsed in TNT for 15 min, and then coverslipped with Aqua-Mount mounting medium. To compare the two detection methods above, we performed preliminary HVC cell counts at similar parasagittal levels and observed that the counts from the chromagen method (n=3 birds) were similar to and fell within two standard deviations of the mean cell counts obtained with the fluorescence method (n=9 birds).

We note that our *in situ* hybridization protocol resulted in strong cellular signal with a typical doughnut-shaped cytoplasmic distribution around a clear area that corresponds to the nucleus (Fig. 1A). We verified this by counterstaining a subset of the sections reacted for the

chromagen detection system with the nuclear stain Hoechst (Fig. 1B). We also note that for both detection protocols the tissue background (diffuse signal in the tissue space between labeled cell somata) was very low so that labeled cells could be clearly identified and counted. Finally, our *in situ* data for areas other than HVC/paraHVC were entirely consistent with our previous descriptions of *zRalDH* mRNA distribution in the zebra finch brain (Denisenko-Nehrbass et al, 2000), including high expression in the anterior nidopallium, peaking in the medial and lateral parts of the anterior magnocellular nucleus (MMAN and LMAN), and in the hyperpallium (Fig. 2A-C).

Mapping

Brains were mapped by a single examiner blind to the identity of the sections being mapped. Mapping was conducted under 40X and 100X magnifications using a Nikon E-600 microscope equipped for brightfield, epifluorescence and darkfield illumination, containing a X-Y-Z stage encoder (Ludl Electronic Products, Ltd.), and yoked through a Lucivid-illuminated camera lucida extension to a microcomputer equipped with Neurolucida software (Microbright Field, Inc.). We used Neurolucida's Contour Mapping capability to draw the outlines and we recorded major structural landmarks such as laminae and commissures from sections processed for *in situ* hybridization for *zRalDH* and visualized under darkfield illumination. We defined *zRalDH*-labeled cells as those with a cytoplasmic distribution of labeling and a clear central area corresponding to the cell nucleus, as determined by counterstaining select sections for nuclear labeling with Hoechst; the typical distribution of the labeling was most often doughnut-shaped (Fig. 1B). We also note that the signal to background ratio in our preparations was very high and labeled cells could be unambiguously identified under the microscope by different observers. The location of *zRalDH*-positive cells was recorded manually with point markers and the associated X-Y coordinates detected by the stage encoders were automatically stored in Neurolucida. The maps were saved as individual MicroBrightField ascii files and later converted to tiff images for figure composition in Adobe Illustrator CS4. Photomicrographs were also recorded with Neurolucida software, saved as tiff images, and contrast enhanced in Adobe Photoshop CS4 for figures.

We tabulated cell counts along the medial-lateral axis at 0.2 mm intervals with Neuroexplorer (v. 4.01.1, MBF). We used the Abercrombie correction factor for large structures in thin sections to more accurately estimate the true cell number per section (Guillery, 2002), where the tabulated counts were multiplied by the ratio (T/T+d = 0.31), where T is the section thickness (10 μm) and d is the average cell diameter (22.1±2.1 μm, n = 20) of randomly chosen *zRalDH*-positive cells with the characteristic doughnut-shaped distribution of *zRalDH* labeling. We also measured the cross-sectional area of HVC or paraHVC that is occupied by *zRalDH*-positive cells by drawing a tight contour around this region in the parasagittal sections. To estimate total number of cells in the combined HVC/paraHVC we used a Cavalieri approach whereby the estimated true number of cells per section counted was multiplied by the interval between the sections counted (0.2 mm). We used a comparable approach to estimate the volume of the HVC/paraHVC. Specifically we multiplied the cross-sectional area occupied by *zRalDH*-positive cells times the sampling interval. We also performed the analysis above separately for paraHVC, medial HVC and lateral HVC. The separation between paraHVC and medial HVC was based on the distribution of retrogradely-labeled cells resulting from injections targeted at RA and the inflection point of the distribution curves of *zRalDH*-labeled cells in paraHVC and medial HVC. The separation between medial and lateral divisions HVC was set at 2.0 mm lat, corresponding to the maximal dorsal-ventral diameter and the peak value of the cross-sectional area occupied by *zRalDH*-labeled cells along the medial-lateral axis (see Fig. 7B in Results). We note that this division into medial and lateral HVC was done solely to facilitate

a more refined regional analysis, without implying a corresponding functional significance; we also note that medial and lateral HVC defined based on these criteria have approximately the same extent in the medial-to-lateral axis. For each section analyzed we also calculated the dorsal-ventral thickness of the region occupied by *zRalDH*-positive cells. This measurement was taken by drawing a line perpendicular to the ventricular zone across the HVC/paraHVC at its widest thickness. Finally, we note that we chose the parasagittal plane because in our experience the medial portions of paraHVC as seen on some frontal sections appear discontinuous from more lateral parts of paraHVC and from HVC; the parasagittal plane helped ensure that such portions of paraHVC were included in the analysis. In addition, the parasagittal plane allowed us to more clearly observe the relationship between paraHVC and the underlying NCM, a structure that is most clearly defined on parasagittal sections.

Analysis

We used (1) ANOVA to test the effects of age and sex on the response variables such as cell count, HVC/paraHVC volume and dorsal-ventral thickness, and (2) linear regressions to look at how those changes occurred along the medial to lateral axis. Statistical analyses were performed with JMP 7 and significance was accepted at $\alpha = 0.05$. Where appropriate we log (x+1) transformed data before statistical analysis.

Retrograde labeling with DiI

To independently determine the medial-to-lateral extent of RA-projecting cells in HVC, we pressure-injected DiI bilaterally into the RA of four adult male zebra finches, which yielded targeted hits in two birds. Birds were anesthetized with nembutal (50 mg/kg body weight) and connected to a stereotaxic apparatus. Feathers were removed where the skin was opened, and a small window was opened in the skull over the coordinates for RA (−0.5 anterior-posterior, 2.2-2.4 medial-lateral, −2.2-2.5 dorsal-ventral; (Nixdorf-Bergweiler and Bischof, 2007). A glass pipette was lowered into RA and DiI (20-40 nl of 5% DiI in water) was pressure injected. Pipettes were slowly withdrawn over several minutes to minimize leakage along the injection tract and the skin was closed over the incision site with flexible collodion. Birds were allowed to recover under a light and monitored regularly for 24 hours before they were returned to the aviary. One week later birds were decapitated, and the brains were dissected, frozen and sectioned on a cryostat as described above. Sections were evaluated at close intervals for injection placement and the presence of retrogradedly-labeled somata in HVC and paraHVC. Brain drawings and mapping of labeled cells were made at 0.2 mm intervals from the midline using a Neurolucida lucivid, as described above.

Results

zRalDH expression in adult males: defining HVC and paraHVC

zRalDH-positive cells have a distinct labeling over the cytoplasm but not the nuclei (Fig. 1). Consistent with previous work (Denisenko-Nehrbass et al., 2000), adult males had numerous labeled cells in the dorsocaudal nidopallial region where HVC and paraHVC are located, but not in the adjacent auditory shelf area or in NCM (Fig. 2A-C). At the medial-most levels, *zRalDH*-expressing cells were distributed as a thin (1-2 cell-thick) band tightly apposed to the ventricular zone (Fig 2D, 0.5 mm lat). At an intermediate level this band of labeled cells became slightly thicker (5-6 cells) but retained the same shape (Fig. 2E, 0.9 mm lat). More laterally, this area assumed the almond shape typical of song nucleus HVC on parasagittal sections (Fig. 2F, 1.9 mm lat). While the distribution of *zRalDH*-labeled cells matched closely the boundaries of HVC and lateral parts of paraHVC as defined by Nissl staining of parasagittal sections (not shown, but see Fig. 5 in Denisenko et al., 2000), they also enabled the clear visualization of the thin medial-most portion of paraHVC (Fig. 2A) that cannot be

visualized by Nissl staining alone. Overall, these observations suggested that the distribution of *zRalDH*-expressing cells by itself might allow us to differentiate paraHVC and HVC.

To obtain a quantitative assessment of this differential distribution, we mapped and counted *zRalDH*-labeled cells along the parasagittal series (Fig. 3A). *zRalDH*-labeled cells were few close to the midline, increased laterally, peaking at ~1.7-2.1 mm lat, and declined rapidly thereafter. The rate of change in cell counts along the medial-to-lateral axis could be approximately described medially (Fig. 4A, 0.1 to 0.9 mm lat) by the linear function Cell $count_{0.1\text{-}0.9\ mm} = 0.012x - 1.48$ ($R^2 = 0.44$; $p = 0.0014$), where x is the medial-lateral position in mm, and more laterally (Fig. 4A, 1.1 to 1.7 mm lat) by the function Cell $Count_{1.1\text{-}1.7\ mm} = 0.036x - 23.83$ ($R^2 = 0.50$; $p = 0.0022$). In the latter segment, cell number increased ~3 times faster than more medially ($P = 0.01$), the pivotal point occurring at ~0.9-1.1 mm lat.

The area occupied by *zRalDH*-expressing cells (Figs. 2A and 3B), defined by the contour that encompasses these cells at each parasagittal level, increased along the medial-to-lateral axis (Fig. 4B, 0.1 to 0.9 mm lat) according to the linear function $Area_{0.1\text{-}0.9\ mm} = 5.87e^{-5}x - 0.0037$ ($R^2 = 0.40$, $p = 0.0026$). More laterally (Fig. 4B, 0.9 to 1.7 mm lat), the area increased ~3.9 times more sharply and could be described by the function $Area_{0.9\text{-}1.7\ mm} = 2.31e^{-4}x - 0.16$ ($R^2 = 0.55$, $p = 0.001$). It reached a maximum between ~1.9-2.1 mm and declined thereafter. The thickness (largest diameter) of the area occupied by *zRalDH*-expressing cells (Fig. 4C) changed little medially (0.3 to ~1 mm lat), but markedly more laterally (~1 to 2 mm lat), peaking at ~2 mm and declining thereafter (Fig. 4C).

This quantitative analysis demonstrates that two distinct segments can be clearly defined based entirely on the numbers and spatial distribution of *zRalDH*-labeled cells. We next examined whether the transition between the medial and lateral segments above might correspond to the medial boundary of the domain containing RA-projecting neurons, thus representing the paraHVC/HVC boundary. For this purpose, we injected adult male finches with DiI into RA and mapped the resulting retrogradely-labeled RA-projecting cells in parasagittal sections. We obtained very good RA hits in two birds, and show one case in Fig 3B. Large numbers of RA-projecting cells can be seen laterally within HVC, but terminate at ~1.1 mm lat (1.0 mm in the case shown in Fig. 3B and 1.2 mm in the other case examined), thus on average just slightly lateral to the transition in the distribution of *zRalDH*-positive cells. These results are consistent with the previous placement of the medial boundary of HVC at ~1.0 mm from the midline, based on Nissl staining in frontal sections (Foster and Bottjer, 1998). We thus propose that the transition in the number and distribution of *zRalDH*-labeled cells marks the boundary between the paraHVC region medially and HVC proper laterally.

Sex differences of HVC as revealed by *zRalDH* expression

As expected, both the number of *zRalDH*-labeled cells and their distribution in the caudodorsal nidopallium were much more restricted in females, who normally do not sing, than in males (Figs. 3A and 4A-B), confirming a preliminary observation (Denisenko-Nehrbass et al., 2000). In contrast to the non-distinct definition of female HVC as seen under Nissl (Fig. 5B; see also Fortune and Margoliash 1995), *zRalDH*-expressing cells were clearly visible, providing a distinct histochemical definition for female HVC (Fig. 5A),. We also observed *zRalDH*-expressing cells in females at the same levels along the medial-lateral axis as in male HVC (Fig. 3A; 1.1 to 2.3 mm lat) but not in the medial-most region occupied by paraHVC in males (<1.1 mm lat).

Total cell count in female HVC differed from male HVC (paraHVC excluded) by ~6x ($p < 0.001$; 765 ± 213 in females vs. 4,560 ± 497 cells in males). The volume occupied by

zRalDH-positive cells in female HVC (0.051 ±0.013 mm^3) was ~16% that of males (0.31 ± 0.024 mm^3; $p < 0.0001$, t-test). In males and females maximum cell count and peak HVC cross-sectional area occurred at the same level along the medial-to-lateral axis (i.e. 2.1 mm lat; Fig. 4). . In sum, based on *zRalDH* expression females lack a paraHVC but appear to possess an HVC that is much more elongated along the medial-to-lateral axis than previously suspected based on Nissl staining.

Distribution of *zRalDH* in paraHVC and HVC during the song learning period

To determine whether there are changes in the distribution of *zRalDH*-cells in HVC and paraHVC regions associated with song learning, we counted and mapped *zRalDH*-expressing cells in parasagittal section series from juvenile males for comparison with adult males. We first note that *zRalDH*-labeling at all juvenile ages examined provided a much sharper and clearer definition of HVC than what can be seen on Nissl-stained sections (Fig. 5C and D). In addition, it allowed us to identify paraHVC in juveniles at parasagittal levels where this structure could not be easily defined based on Nissl staining alone (Fig. 5E and F).

The structural pattern described for adults was similar for juveniles, with a medial thin band corresponding to paraHVC, a thicker lateral region corresponding to HVC proper, and a transition point at ~0.9-1.1 mm lat (Fig. 6). However, at 20 dph no *zRalDH*-labeled cells were observed at the medial-most levels (0.1-0.5 mm), indicating that paraHVC does not extend as far medially at younger ages compared to older ages. We then conducted quantitative age comparisons separately for paraHVC, and for HVC, subdividing the latter into medial and lateral sectors at the level where cross-sectional area is greatest (see Methods for details and Table 1 for statistics). For paraHVC, we found age differences in the total number of *zRalDH*-positive cells (Figs. 6A, 7A) and in cross-sectional area (Fig. 6B) and volume (Fig. 7B). *Post-hoc* examination (Tukey-Kramer test) revealed that the 20 dph birds had the fewest *zRalDH*-positive cells and lowest paraHVC volume while the 50 dph birds had the highest estimates and adults and 35 dph birds had intermediate estimates for both parameters (Fig. 7A and B). A significant difference was also seen in medial HVC for *zRalDH*-positive cell counts (Figs. 6A, 7C), but not for volume (Figs. 6B, 7D). Similar trends were seen in lateral HVC, for cell counts (Fig. 6A, 7E) and volume (Fig. 6B, 7F) but did not reach significance, suggesting that the latter region is more constrained throughout juvenile development. The thickness of the cross-sectional area occupied by *zRalDH*-positive cells did not significantly vary with age (Fig. 6C) within the paraHVC, medial or lateral HVC.

In summary, in males from 20 dph to 50 dph the *zRalDH*-positive cell numbers increase roughly 77% across the entire paraHVC-HVC axis, from ~3600 to ~6400 cells. Then cell numbers decline by ~30% from the peak 50 dph cell counts to adult numbers. This represents a net addition of roughly 900 mature area X-projecting cells during male adolescence.

Discussion

Using expression analysis of *zRalDH*, a key component in the metabolic pathway of vitamin A and a marker of X-projecting neurons in song nucleus HVC, we have revealed novel insights into the organization and ontogenesis of HVC and paraHVC in zebra finches. Our data provide a precise definition of paraHVC in adult and juvenile males, evidence that the populations of *zRalDH*-expressing neurons in both HVC and paraHVC undergo dynamic changes in concert with the period of song learning in juvenile males, and novel aspects about sex differences in these key components of the song system. Our approach was particularly valuable for visualizing these regions in juveniles, where the song system is not

yet mature, and in females, where song nuclei are largely regressed in comparison with males. More generally, our study shows how the analysis of a molecular marker can help to identify and characterize parts of the oscine song system that are not immediately clear or visible using cytoarchitectonic criteria. Our approach also avoided the uncertainties of counting and mapping retrogradely-labeled cells resulting from the injection of tract-tracers (e.g., incomplete targeting of a large nucleus like area X) for quantitative assessments of specific song control areas. Finally, since *zRalDH* is the main enzyme responsible for the generation of retinoic acid, our results provide further evidence consistent with a role of retinoids in modulating the development of the song system and singing behavior.

We observed a good correspondence between tract-tracing (distribution of HVC's RA-projecting cells) and molecular criteria (number and distribution of *zRalDH*-expressing cells) for defining the HVC/paraHVC transition. This demonstrates the usefulness of a molecular approach to distinguish these two structures without the need for multiple markers or the more labor-intensive and variable tract-tracing approach. Based on our combined data, we propose that the HVC/paraHVC boundary lies at ~1.0-1.1 mm lat. Medial to this level, paraHVC is a thin band that overlies auditory region NCM and contains X-projecting but not RA-projecting cells. Lateral to this level, HVC-proper is a much thicker structure with a distinct ovoid shape. It contains much higher numbers of X-projecting cells as well as RA-projecting cells, and its characteristic cytoarchitectonic features can be readily visualized by Nissl, even on thin sections. These observations are consistent with the notion that paraHVC is a distinct region of the song system, with specific cytoarchitectonic, molecular, and possibly physiological properties, as suggested in Foster and Bottjer (1998), rather than simply a medial extension of HVC.

Previous studies suggest that expression of the estrogen receptor (ER) is a useful marker for defining HVC and paraHVC in songbirds. Indeed, ER-expressing cells are present in the HVC and paraHVC of canaries (Gahr et al., 1993; Johnson and Bottjer, 1995; Metzdorf et al., 1999) and constitute a useful marker for defining these areas in this species, In contrast, estrildinae finches like the zebra finch have much lower densities (~20%) of ER-expressing cells in HVC (Gahr et al., 1993; see their figure 3a and b), Furthermore, the nidopallial shelf region ventral to HVC and the NCM region ventral to paraHVC of zebra finches also contain considerable numbers of ER-expressing cells (Gahr et al., 1993; Saldanha and Coomaralingam, 2005; Lovell and Mello, unpublished observations). European starlings show yet another distinct pattern, with high ER expression in paraHVC and only low to moderate expression in HVC (Bernard et al., 1999). Overall, these observations illustrate important species differences in the distribution of ER-expressing cells among songbirds, and indicate that this trait is not a useful marker for defining paraHVC in the zebra finch. This is in sharp contrast to *zRalDH*, which is highly expressed in HVC and paraHVC but absent in the neighboring areas of the zebra finch brain.

Male and female HVC

Our results demonstrate a clear sex dimorphism in the number of *zRalDH*-expressing cells in HVC, consistent with previous descriptions of a major sex dimorphism based on broad cytoarchitectonic features of zebra finch HVC (Fortune and Margoliash, 1995; Nottebohm and Arnold, 1976; Wade and Arnold, 2004). More importantly, we show that a paraHVC region is clearly lacking in adult females. We also show that *zRalDH*-expressing cells in females, although much fewer than in males, extend beyond the identifiable HVC based on Nissl staining to cover a medial-to-lateral range that is comparable to that of male HVC. In sum, *zRalDH* expression has provided a more comprehensive definition of female HVC.

Since female zebra finches lack a striatal area X, it seems unlikely that the role of *zRalDH*-expressing cells in female HVC is related to a projection of the song system onto the

striatum. Rather, retinoid signaling in female HVC could be involved in autocrine or paracrine regulatory pathways within HVC itself (Jeong et al., 2005). Female zebra finches do not learn to sing but do present perceptual song learning, exhibiting preferences as adults to the songs they heard as juveniles (Clayton, 1990; Leitner and Catchpole, 2002). In addition, lesions that destroy HVC and neighboring auditory regions like the shelf and portions of NCM in female zebra finches result in non-discriminating copulation solicitation displays in response to auditory stimulation (Brenowitz, 1991; MacDougall-Shackleton et al., 1998), suggesting that such lesions disrupt a selectivity filter in the response to ethologically relevant auditory stimuli. It is thus possible that female HVC and its *zRalDH*-expressing cells subserve important roles in perceptual aspects of vocal communication, but this hypothesis requires further testing.

Since adult females lack a paraHVC, NCM in females may lack inputs from this region, and thus may not be under a modulatory influence from the vocal-motor pathways. Such input has been postulated to be present in males, where it might modulate auditory responses to song during singing behavior (Foster and Bottjer, 1998). Perhaps more intriguingly, since *zRalDH* function is to generate retinoic acid that can then act on adjacent brain areas (McCaffery et al., 2006), female NCM would lack a potential source of modulatory action on gene expression and cell differentiation. Preliminary evidence suggests that *zRalDH*-positive cells medial to HVC are present in juvenile females in a distribution similar to that seen in the early juvenile males (Mello and Olson, unpublished observations), suggesting that juvenile females might possess a structure resembling paraHVC, but such cells disappear by adulthood. In any scenario, our results point to novel and interesting avenues for investigating how sex dimorphism in a part of the vocal-motor song pathway may influence perceptual aspects of vocal communication in songbirds.

Development

The song system of zebra finches undergoes considerable change during the song learning period, ranging from changes in the composition and properties of cell populations within song control nuclei to the formation and maturation of the projections across these nuclei (for reviews, see Brenowitz, 1997; Zeigler and Marler, 2004). Our present analysis demonstrates marked changes in the *zRalDH*-expressing cell population within HVC/paraHVC that are concurrent with the vocal learning period. Specifically, the numbers of *zRalDH*-expressing cells in HVC and paraHVC undergo a considerable increase between 20 and 50 dph, declining thereafter to reach adult levels; this change is particularly robust in paraHVC and more marked in medial than lateral HVC.

We have previously shown that *zRalDH*-expressing cells in the HVC of adult zebra finches correspond to X-projecting neurons (Denisenko-Nehrbass et al., 2000), a cell population thought to be primarily formed during embryonic life (Alvarez-Buylla et al., 1988). There are two general explanations for the developmental changes we now describe that cannot be differentiated presently. One possibility is that X-projecting cells in adult HVC and paraHVC are already present in these areas at an early age post-hatch, but at first only a small portion of them expresses *zRalDH*. Cells negative for *zRalDH* would start expressing this gene later on, in conjunction with the maturation of the song system. Although we cannot discard this hypothesis, it would imply that *zRalDH* expression is an indicator of a late maturation stage of X-projecting cells. We find this unlikely since *zRalDH* expression is characteristic of embryonic development (McCaffery and Drager, 2000), reflecting the widespread roles of retinoic acid signaling in various aspects of embryogenesis. Furthermore, previous analysis using radioactive *in situ* hybridization did not detect obvious changes in expression levels of *zRalDH* in HVC as a function of age, song stimulation or singing behavior, suggesting that *zRalDH* expression is a stable property of X-projecting

cells (Denisenko-Nehrbass et al., 2000; and Denisenko-Nehrbass and Mello, unpublished observations).

The other general possibility is that the post-embryonic developmental changes in the *zRalDH*-positive cell counts within HVC/paraHVC largely reflect dynamic changes in cell composition during the period of vocal learning. According to this hypothesis, only a portion of X-projecting neurons would be present in HVC and paraHVC in juveniles at the beginning of the song learning period. Additional *zRalDH*-expressing cells would then migrate from other brain areas, enter HVC and paraHVC, loose their migratory phenotype and become integrated into the song system circuitry as X-projecting neurons. This migration process would result in a net increase in the number of *zRalDH*-expressing cells within HVC/paraHVC during the period from 20 to 50 dph. Thereafter, some *zRalDH*-expressing cells would either die or migrate out of HVC and paraHVC into other brain areas, resulting in a net decrease in the number of *zRalDH*-expressing cells until reaching adult levels. Consistent with this hypothesis, HVC at 20 dph is considerably smaller than at 50 dph, a difference that does not appear to be accounted for by changes in the distribution of HVC soma size (Bottjer et al., 1986). Interestingly, the increases in neuronal cell number that occur in HVC during the song learning period are usually attributed to the incorporation of newly formed RA-projecting neurons, a process that continues well into adulthood (Alvarez-Buylla et al., 1988; Kirn et al., 1991). The migration hypothesis delineated above, however, suggests that some X-projecting cells are also incorporated into HVC/paraHVC during the song learning period and could thus contribute to the overall increase in neuronal cell number in this area, even though these cells were born much earlier during embryonic life. We favor this general migration hypothesis to explain the observed changes the *zRalDH*-positive cell counts during the song learning period, but a conclusive demonstration will require direct evidence that *zRalDH*-expressing cells migrate from other brain areas into HVC and paraHVC.

Compared to HVC, paraHVC lacks RA-projecting cells and could represent a remnant of a primordial structure present in juveniles and that gives rise to adult HVC. Our data, however, are incompatible with this hypothesis. In fact, paraHVC appeared not fully formed at the earliest age examined (20 dph), lacking *zRalDH*-positive cells at the medial-most levels. Instead, this medial part of paraHVC, which is in close proximity to NCM, seems to form at a later age (by 35 dph), in conjunction with the maturation of HVC. It may be particularly important that paraHVC forms during the song learning period, when song auditory memories are being laid down and auditory feedback is critical for song development. Its localization adjacent to NCM could provide access to song-processing circuits that play central roles in the auditory memorization of song. Testing this hypothesis will require direct evidence that paraHVC receives auditory input and is activated by song stimulation. On the other hand, tract-tracing evidence suggests that adult paraHVC might project into NCM (Foster and Bottjer, 1998). It is thus possible that as paraHVC emerges during the song learning period, the vocal-motor circuits exert a growing influence onto NCM, which could have important implications for modulating auditory feedback during singing. Further tract-tracing data and electrophysiological recordings will be required to prove this point.

The anterior forebrain pathway plays key roles in song development, as attested by studies involving lesions or inactivation of area X and/or LMAN during song learning (Bottjer et al., 1984; Foster and Bottjer, 2001; Scharff and Nottebohm, 1991). Furthermore, the local blockade of retinoic acid synthesis by inhibition of *zRalDH* in juvenile HVC disrupts song crystallization (Denisenko-Nehrbass et al, 2000), pointing further to a role of X-projecting neurons in song learning. Thus, our observation that the numbers of *zRalDH*-expressing cells in HVC/paraHVC undergo marked developmental changes may have important

functional consequences. For example, our findings may reflect an increase in the synaptic input area X receives from HVC during a period of high vocal plasticity, followed by a decline in such input as song matures and the role of the anterior forebrain pathway in vocal plasticity becomes more restricted in adults (Kao et al., 2005). Alternatively, our observations may reflect developmental fluctuations in the amount of retinoic acid available to area X from HVC sources. Under either scenario, further analysis of developmental changes in HVC's input to its striatal target may reveal further insights into the role of this projection system in vocal development.

zRalDH is the terminal enzyme in the synthetic pathway for retinoic acid. In juveniles, blockade of retinoic acid synthesis by pharmacological inhibition of *zRalDH* activity markedly disrupts song crystallization (Denisenko-Nehrbass et al., 2000). Similarly, supplementation with excess dietary retinoic acid during the song learning period results in songs that are highly variable, with frequent omission or addition of song elements (Wood et al., 2008). Thus it is clear that a careful balance in retinoid signaling is necessary for the correct timing of neuronal plasticity during the development of learned song, similar to other retinoic acid-dependent brain functions (McCaffery et al., 2003). In general, adequate retinoic acid levels in brain tissues are thought to be achieved by maintaining a narrow balance of retinoic acid synthesis and degradation, and age-related changes in *zRalDH* expression that we report here may be necessary to modulate neuronal plasticity during development. While retinoic acid signaling has been defined in terms of its effects on neuronal phenotypes in rodents (Haskell et al., 2002), the specific role of retinoic acid on the avian song system is not known, although some evidence of specific gene regulation within the song system in the context of retinoid manipulations is beginning to emerge (Wood et al., 2008).

In sum, using a molecular marker, *zRalDH*, we have shown here that the population of X-projecting neurons in HVC and paraHVC undergoes substantial changes during the zebra finch song development period. Furthermore, this marker identifies the structural boundaries of HVC and paraHVC particularly well in brains that have poor cytoarchitectural definition, such as in juveniles and females (Fig. 5). This observation helped demonstrate that female zebra finches have a larger HVC than previously recognized, but that they lack a paraHVC region. Further investigation into the role of retinoid signaling in the development of the avian song system in both males and females will enhance our understanding of vocal and auditory learning.

Acknowledgments

This work was supported by NIH grants 2R01-DC002853 and F32-NS062609. Assistance in collecting images came from Anda Cornea at the Neuroscience Imaging Center at OHSU, supported by NIH grant (P30-NS06180; Aicher, P.I.). We would like to thank Peter Lovell and Katy Horback for thoughtful discussion and technical assistance, and we thank two anonymous reviewers for their valuable feedback.

Contract grant sponsors: NIH/NIDCD and NIH/NINDS; contract grant numbers: 2R01-DC002853, 1F32-NS062609.

Literature Cited

Alvarez-Buylla A, Garcia-Verdugo JM, Mateo AS, Merchant-Larios H. Primary neural precursors and intermitotic nuclear migration in the ventricular zone of adult canaries. J of Neurosci. 1998; 18:1020–1037. [PubMed: 9437023]

Alvarez-Buylla A, Theelen M, Nottebohm F. Birth of projection neurons in the higher vocal center of the canary forebrain before, during, and after song learning. Proc Natl Acad Sci U S A. 1988; 85:8722–8726. [PubMed: 3186755]

Bernard DJ, Bentley GE, Balthazart J, Turek FW, Ball GF. androgen receptor, estrogen receptor {alpha}, and estrogen receptor {beta} show distinct patterns of expression in forebrain song control nuclei of European starlings. Endocrinology. 1999; 140:4633–4643. [PubMed: 10499520]

Bolhuis JJ, Hetebrij E, Boer-Visser AMD, Groot JHD, Zijlstra GGO. Localized immediate early gene expression related to the strength of song learning in socially reared zebra finches. Eur J Neurosci. 2001; 13:2165–2170. [PubMed: 11422458]

Bolhuis JJ, Zijlstra GGO, den Boer-Visser AM, Van der Zee EA. Localized neuronal activation in the zebra finch brain is related to the strength of song learning. Proc Natl Acad Sci U S A. 2000; 97:2282–2285. [PubMed: 10681421]

Bottjer S, Halsema K, Brown S, Miesner E. Axonal connections of a forebrain nucleus involved with vocal learning in zebra finches. J Comp Neurol. 1989; 279:312–326. [PubMed: 2464011]

Bottjer SW, Miesner EA, Arnold AP. Forebrain lesions disrupt development but not maintenance of song in passerine birds. Science. 1984; 224:901–903. [PubMed: 6719123]

Bottjer SW, Miesner EA, Arnold AP. Changes in neuronal number, density and size account for increases in volume of song-control nuclei during song development in zebra finches. Neurosci Lett. 1986; 67:263–268. [PubMed: 3737014]

Brenowitz E. Altered perception of species-specific song by female birds after lesions of a forebrain nucleus. Science. 1991; 251:303–305. [PubMed: 1987645]

Brenowitz EA. Comparative approaches to the avian song system. J Neurobiol. 1997; 33:517–531. [PubMed: 9369457]

Clayton DF. Role of gene regulation in song circuit development and song learning. J Neurobiol. 1997; 33:549–571. [PubMed: 9369459]

Clayton N. Subspecies recognition and song learning in zebra finches. Anim Behav. 1990; 40:1009–1017.

Denisenko-Nehrbass NI, Jarvis E, Scharff C, Nottebohm F, Mello CV. Site-specific retinoic acid production in the brain of adult songbirds. Neuron. 2000; 27:359–370. [PubMed: 10985355]

Doupe AJ, Kuhl PK. Birdsong and human speech: common themes and mechanisms. Ann Rev Neurosci. 1999; 22:567–631. [PubMed: 10202549]

Fortune ES, Margoliash D. Parallel pathways and convergence onto HVc and adjacent neostriatum of adult zebra finches (*Taeniopygia guttata*). J Comp Neurol. 1995; 360:413–441. [PubMed: 8543649]

Foster EF, Bottjer SW. Axonal connections of the high vocal center and surrounding cortical regions in juvenile and adult male zebra finches. J Comp Neurol. 1998; 397:118–138. [PubMed: 9671283]

Foster EF, Bottjer SW. Lesions of a telencephalic nucleus in male zebra finches: Influences on vocal behavior in juveniles and adults. J Neurobiol. 2001; 46:142–165. [PubMed: 11153015]

Gahr M, Güttinger HR, Kroodsma DE. Estrogen receptors in the avian brain: survey reveals general distribution and forebrain areas unique to songbirds. J Comp Neurol. 1993; 327:112–122. [PubMed: 8432903]

Griffiths R, Double MC, Orr K, Dawson RJG. A DNA test to sex most birds. Mol Ecol. 1998; 7:1071–1075. [PubMed: 9711866]

Guillery RW. On counting and counting errors. J Comp Neurol. 2002; 447:1–7. [PubMed: 11967890]

Haskell GT, Maynard TM, Shatzmiller RA, LaMantia A. Retinoic acid signaling at sites of plasticity in the mature central nervous system. J Comp Neurol. 2002; 452:228–241. [PubMed: 12353219]

Jeong JK, Velho TAF, Mello CV. Cloning and expression analysis of retinoic acid receptors in the zebra finch brain. J Comp Neurol. 2005; 489:23–41. [PubMed: 15977168]

Johnson F, Bottjer SW. Differential estrogen accumulation among populations of projection neurons in the higher vocal center of male canaries. J Neurobiol. 1995; 26:87–108. [PubMed: 7714528]

Kao MH, Brainard MS. Lesions of an avian basal ganglia circuit prevent context-dependent changes to song variability. J Neurophysiol. 2006; 96:1441–1455. [PubMed: 16723412]

Kim Y-H, Arnold AP. Distribution and onset of retinaldehyde dehydrogenase (zRalDH) expression in zebra finch brain: Lack of sex difference in HVC and RA at early posthatch ages. J Neurobiol. 2005; 65:260–268. [PubMed: 16155902]

Kirn JR, Alvarez-Buylla A, Nottebohm F. Production and survival of projection neurons in a forebrain vocal center of adult male canaries. J Neurosci. 1991; 11:1756–1762. [PubMed: 2045885]

Kirn JR, DeVoogd T. Genesis and death of vocal control neurons during sexual differentiation in the zebra finch. J Neurosci. 1989; 9:3176–3187. [PubMed: 2795159]

Kirn JR, Fishman Y, Sasportas K, Alvarez-Buylla A, Nottebohm F. Fate of new neurons in adult canary high vocal center during the first 30 days after their formation. J Comp Neurol. 1999; 411:487–494. [PubMed: 10413781]

Leitner S, Catchpole CK. Female canaries that respond and discriminate more between male songs of different quality have a larger song control nucleus (HVC) in the brain. J Neurobiol. 2002; 52:294–301. [PubMed: 12210096]

London SE, Clayton DF. Functional identification of sensory mechanisms required for developmental song learning. Nat Neurosci. 2008; 11:579–586. [PubMed: 18391944]

MacDougall-Shackleton S, Hulse SH, Ball GF. Neural bases of song preferences in female zebra finches (*Taeniopygia guttata*). NeuroReport. 1998; 9:3047–3052. [PubMed: 9804314]

Mello CV, Jarvis ED, Denisenko N, Rivas M. Isolation of song-regulated genes in the brain of songbirds. Methods Mol Biol. 1997; 85:207–217.

McCaffery P, Drager UC. Regulation of retinoic acid signaling in the embryonic nervous system: a master differentiation factor. Cytokine Growth Factor Rev. 2000; 11:233–249. [PubMed: 10817966]

McCaffery P, Zhang J, Crandall JE. Retinoic acid signalling and function in the adult hippocampus. J Neurobiol. 2006; 66:780–791. [PubMed: 16688774]

McCaffery PJ, Adams J, Maden M, Rosa-Molinar E. Too much of a good thing: retinoic acid as an endogenous regulator of neural differentiation and exogenous teratogen. Eur J Neuroscience. 2003; 18:457–472.

Metzdorf R, Gahr M, Fusani L. Distribution of aromatase, estrogen receptor, and androgen receptor mRNA in the forebrain of songbirds and nonsongbirds. J Comp Neurol. 1999; 407:115–129. [PubMed: 10213192]

Napoli JL. Interactions of retinoid binding proteins and enzymes in retinoid metabolism. Biochim Biophys Acta. 1999; 1440:139–162. [PubMed: 10521699]

Nixdorf-Bergweiler, BE.; Bischof, H-J. A stereotaxic atlas of the brain of the zebra finch, *Taeniopygia guttata*, with special emphasis on telencephalic visual and song system nuclei in transverse and sagittal sections. National Library of Medicine (US), National Center for Biotechnology Information; Bethesda (MD): 2007.

Nottebohm F, Arnold A. Sexual dimorphism in vocal control areas of the songbird brain. Science. 1976; 194:211–213. [PubMed: 959852]

Nottebohm F, Stokes TM, Leonard CM. Central control of song in the canary, *Serinus canarius*. J Comp Neurol. 1976; 165:457–486. [PubMed: 1262540]

Ölveczky BP, Andalman AS, Fee MS. Vocal experimentation in the juvenile songbird requires a basal ganglia circuit. PLoS Biol. 2005; 3:902–909.

Phan ML, Pytte CL, Vicario DS. Early auditory experience generates long-lasting memories that may subserve vocal learning in songbirds. Proc Natl Acad Sci U S A. 2006; 103:1088–1093. [PubMed: 16418265]

Reiner A, Perkel DJ, Mello CV, Jarvis ED. Songbirds and the revised avian brain nomenclature. Ann N Y Acad Sci. 2004; 1016:77–108. [PubMed: 15313771]

Saldanaha CJ, Coomaralingam L. Overlap and co-expression of estrogen synthetic and responsive neurons in the songbird brain—a double-label immunocytochemical study. Gen Comp Endocrinol. 2005; 141:66–75. [PubMed: 15707604]

Scharff C, Nottebohm F. A comparative study of the behavioral deficits following lesions of various parts of the zebra finch song system: implications for vocal learning. J Neurosci. 1991; 11:2896–2913. [PubMed: 1880555]

Scott BB, Lois C. Developmental origin and identity of song system neurons born during vocal learning in songbirds. J Comp Neurol. 2007; 502:202–214. [PubMed: 17348018]

Sohrabji F, Nordeen EJ, Nordeen KW. Selective impairment of song learning following lesions of a forebrain nucleus in the juvenile zebra finch. Behav Neural Biol. 1990; 53:51–63. [PubMed: 2302141]

Velho TAF, Lovell P, Mello CV. Enriched expression and developmental regulation of the middle-weight neurofilament (NF-M) gene in song control nuclei of the zebra finch. J Comp Neurol. 2007; 500:477–497. [PubMed: 17120287]

Wada K, Howard JT, McConnell P, Whitney O, Lints T, Rivas MV, Horita H, Patterson MA, White SA, Scharff C, Haesler S, Zhao S, Sakaguchi H, Hagiwara M, Shiraki T, Hirozane-Kishikawa T, Skene P, Hayashizaki Y, Carninci P, Jarvis ED. A molecular neuroethological approach for identifying and characterizing a cascade of behaviorally regulated genes. Proc Natl Acad Sci U S A. 2006; 103:15212–15217. [PubMed: 17018643]

Wade J, Arnold AP. Sexual differentiation of the zebra finch song system. Proc Natl Acad Sci U S A. 2004; 1016:540–559.

Wilbrecht L, Williams H, Gangadhar N, Nottebohm F. high levels of new neuron addition persist when the sensitive period for song learning is experimentally prolonged. J Neurosci. 2006; 26:9135–9141. [PubMed: 16957070]

Wild JM. Neural pathways for the control of birdsong production. J Neurobiol. 1997; 33:653–670. [PubMed: 9369465]

Wissman AM, Brenowitz EA. the role of neurotrophins in the seasonal-like growth of the avian song control system. J Neurosci. 2009; 29:6461–6471. [PubMed: 19458217]

Wood WE, Olson CR, Lovell PV, Mello CV. Dietary retinoic acid affects song maturation and gene expression in the song system of the zebra finch. Dev Neurobiol. 2008; 68:1213–1224. [PubMed: 18548487]

Zeigler HP, Marler P. Behavioral Neurobiology of Birdsong. Ann N Y Acad Sci. 2004; 1016:1–786. [PubMed: 15313767]

Zeigler, HP.; Marler, P. Neuroscience of Birdsong. Cambridge University Press; Cambridge: 2008.

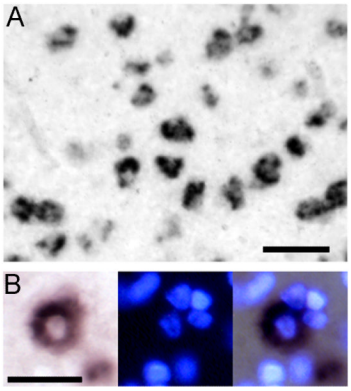

Figure 1.
A. *zRalDH*-positive cells in HVC show distinct cellular labeling; scale bar = 0.05 mm. B. Detail views of cellular labeling pattern under brightfield (left), UV illumination (center) and merged image. At the center of the field is a *zRalDH*-positive cell with characteristic cytoplasmic distribution of labeling and a clear central zone; the nuclei of the labeled cell and of neighboring -negative cells are readily identifiable by Hoechst staining; scale bar = 0.025 mm.

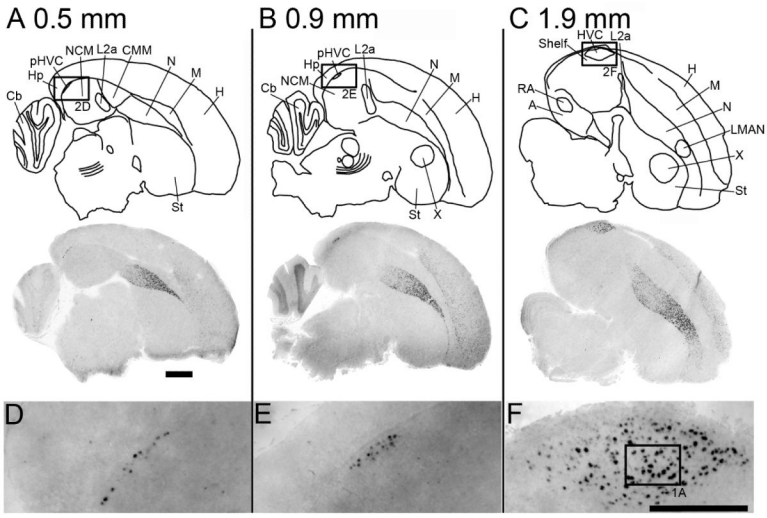

Figure 2.

zRalDH expression in serial parasagittal sections of an adult male zebra finch brain (A. 0.5 mm, B. 0.9 mm and C. 1.9 mm lat); scale bar = 1.0 mm. Diagrams on top are camera lucida drawings of the respective Nissl-stained adjacent sections. Images below show composite bright field photographs of brain sections hybridized with an antisense *zRalDH* riboprobe; LMAN is indicated in C, MMAN is not shown. (D-F) ParaHVC to HVC images of boxed regions in A-C, respectively; scale bar = 0.5 mm. Abbreviations for brain regions: A, arcopallium; Cb, cerebellum; CMM, caudomedial mesopallium; H, hyperpallium; Hp, hippocampus; HVC, nucleus HVC of the nidopallium; L2a, subfield L2a of field L; LMAN, lateral magnocellular nucleus of the anterior nidopallium; M, mesopallium; N, nidopallium; NCM, caudomedial nidopallium; pHVC, paraHVC; RA; robust nucleus of the arcopallium; St, striatum; X, Area X of the medial striatum.

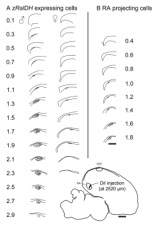

Figure 3.

Reconstruction of HVC and paraHVC in parasagittal section series based on distribution of *zRalDH*-labeled cells or RA-projecting cells. A. Mapping of *zRalDH*-labeled cells for a representative adult male and female; *zRalDH* expression occurs more medially into paraHVC in the male, but not the female. (B) Mapping of retrogradely-labeled cells resulting from DiI injection into RA in an adult male. Labeled cells occur within HVC but not paraHVC, Injection site location is indicated on the brain drawing at the bottom right. For all panels, sections are taken. at 0.2 mm intervals beginning at the midline (reference = 0); scale bar = 0.5 mm.

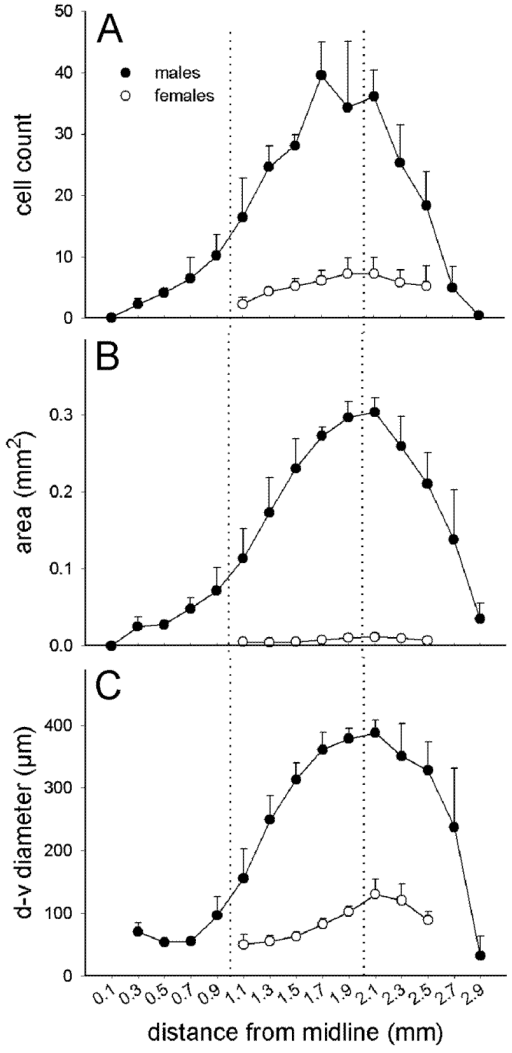

Figure 4.

Medial-to-lateral progression of para-HVC/HVC traits in parasagital brain sections from adult male (solid symbols) and female (open symbols) zebra finches. A. average cell count per 10 μm section, B. cross sectional area occupied by *zRalDH*-positive cells, C. diameter of the cross sectional area occupied by *zRalDH*-positive cells along the dorsal-ventral axis. The dotted lines mark the approximate transition between HVC and paraHVC (left) and the approximate peak size of the HVC (right). Error bars represent ±1SE for group means.

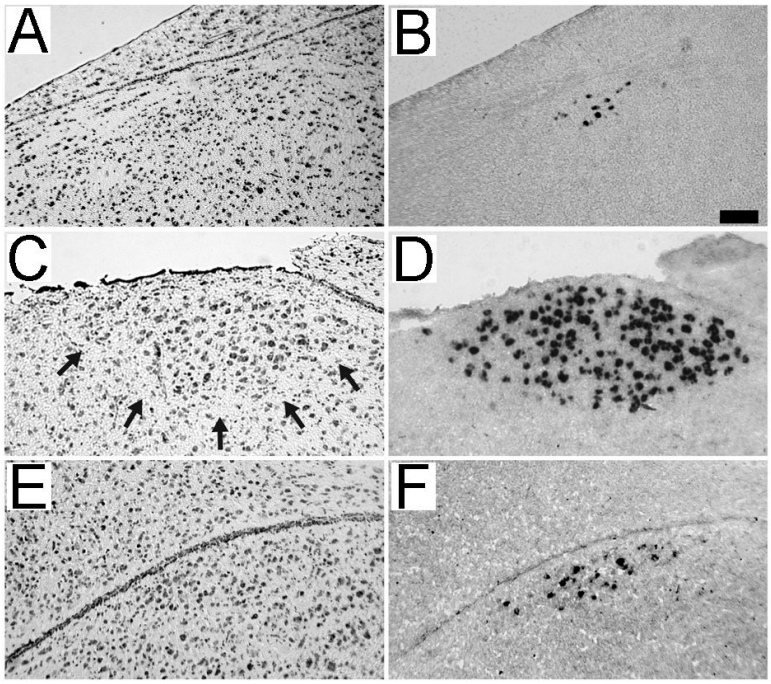

Figure 5.

Comparison of Nissl staining and *zRalDH* labeling. Shown are adjacent parasagittal brain sections from an adult female at the level of HVC (A and B; ~2 mm lat) and from a juvenile (20 dph) male at the level of HVC (C and D; ~2 mm lat) and paraHVC (E and F; ~0.9 mm lat). Sections were stained for Nissl (A, C and E) or processed for *zRalDH in situ* hybridization (B, D and F). Arrows in panel C denote the ventral boundary of HVC that is characteristic of Nissl-stained sections of male brains. In contrast, HVC in females (panel A) and paraHVC in juvenile males (panel E) are not readily visible under Nissl. Scale bar = 0.025 mm.

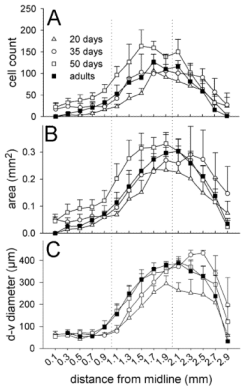

Figure 6.

Effects of age on the lateral progression of para-HVC and HVC traits for 4 age categories (adult data are re-plotted from Fig. 4 to facilitate comparisons): adult males (solid symbols), 20-day old males (open triangles), 35-day old males (open circles) and 50-day old males (open squares). A. Average cell count per 10 μm section, B. Cross-sectional area occupied by *zRalDH*-positive cells, C. Diameter of the cross sectional area occupied by *zRalDH*-positive cells measured along the dorsal-ventral axis. The dotted lines mark the approximate transition between HVC and paraHVC (left) and the approximate peak size of the HVC (right). Error bars represent ±1SE.

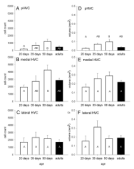

Figure 7.

Age-related effects in zebra finches on the number of *zRalDH*-positive cells (A, C, E) and the volume of the structure occupied by *zRalDH*-positive cells along the medial-lateral gradient from paraHVC (A, B) the medial portion of HVC (C, D) and the lateral portion of HVC (E, F). Age groups that do not share the same letter are significantly different based on Tukey-Kramer HSD comparisons. Error bars represent ±1SE.

Table 1

ANOVA statistics for age-related differences in male zebra finches in total *zRalDH*-labeled cell counts, reconstructed volumes, and dorsal-ventral thickness of paraHVC, medial HVC and lateral HVC regions. Cell counts and volumes were measured over the regions 0-1mm, 1-2 mm and 2-3 mm from the midline for paraHVC, medial HVC and lateral HVC, respectively. Dorsal-ventral thickness was measured at 0.5, 1.5 and 2.5 mm for paraHVC, medial HVC and lateral HVC, respectively

		$F_{3,11}$ =	p =
Cell Count	paraHVC	3.80	0.04
	medial HVC	3.78	0.04
	lateral HVC	0.37	0.78
Volume	paraHVC	4.60	0.03
	medial HVC	1.98	0.18
	lateral HVC	1.93	0.18
Dorsal-ventral thickness	paraHVC	1.70	0.23
	medial HVC	1.73	0.22
	lateral HVC	1.12	0.39